blending with Profax (Table V, ref 1). Further, the portion that was still soluble had an η_{inh} = 1.40. Thus, the insolubilized portion was much higher in molecular weight and would have had a larger number of isotactic blocks per chain.

The NMR rigidity results also revealed differences attributable to block size distributions. Cooling the solution of the ether-soluble fraction from 135 °C to room temperature reduced the observed isotactic pentad fraction 20%, whereas the decrease was 40% for the hexane-soluble fraction. The difference is an indication of a higher proportion of crystallizable blocks, i.e., there are more of the longer isotactic blocks in the hexane-soluble fraction.

Acknowledgment. Dr. H. Thielke and Ralph Fuller provided X-ray and GPC measurements, respectively. The NMR rigidity measurements were suggested and first tested by Dr. Fred Davidson. Helpful discussions with Profs. B. Wunderlich and U. Suter are gratefully acknowledged.

Registry No. ELPP, 9003-07-0.

References and Notes

(1) Collette, J. W.; Tullock, C. W.; MacDonald, R. N.; Buck, W. H.; Su, A. C. L.; Harrell, J. R.; Mulhaupt, R.; Anderson, B. C. Macromolecules, preceding paper in this issue.
(2) Luongo, J. P. *J. Appl. Polym Sci.* **1960**, *3*, 302.
(3) Wunderlich, B. *Macromolecular Physics*; Academic: New York, 1976; Vol. II, p 149; and private conversation.
(4) Asakura, T.; Ando, I.; Nishioka, A.; Doi, Y.; Keii, T. *Makromol. Chem.* **1977**, *178*, 791.
(5) Lindeman, L. P.; Adams, J. Q. *Anal. Chem.* **1971**, *43*, 1245.
(6) Cheng, H. N.; Bennett, M. A. "^{13}C NMR Spectra of Polyolefins". In *Advances in Polyolefins*; Seymour, R. B., Cheng, T., Eds.; Plenum Press: New York, 1987; p 393.
(7) Zambelli, A.; Locatelli, P.; Bajo, G.; Bovey, F. A. *Macromolecules* **1975**, *8*, 687.
(8) Stehling, F. C.; Knox, J. R. *Macromolecules* **1975**, *8*, 595.
(9) Zambelli, A.; Sacchi, M. C.; Locatelli, P. In *Transition Metal Catalyzed Polymerizations*; Quirk, R. P., Ed.; MMI Press Symposium Series, Vol. 4; Harwood Academic Publishers: New York, 1983; p 83.
(10) Doi, Y.; Suzuki, E.; Keii, T. Reference 9, p 737.
(11) Bovey, F. A. *High Resolution NMR of Macromolecules*; Academic Press: New York, 1972.
(12) Harwood, H. J. *J. Polym Sci, Part C* **1968**, *25*, 37; and private communications.
(13) Groenewege, M. P.; Schuyer, J.; Smidt, J.; Tuijnman, C. A. "Crystalline Olefin Polymers". In *High Polymers*; Raff, R. A. V., Doak, K. W., Eds.; Interscience: New York, 1965; Vol. XX, Part 1, pp 795–811.
(14) Cowie, J. M. G. *Eur. Polym. J.* **1973**, *91*, 1041.
(15) Aggarwal, S. L. In *Polymer Handbook*, 2nd Ed.; Bandrup, J., Immergut, E. H., Eds.; John Wiley & Sons: New York, 1975; p V-23.
(16) Lauritzen, J. I., Jr.; Hoffman, J. *J. Chem. Phys.* **1959**, *31*, 1680; *J. Res. Natl. Bur. Stand.* **1959**, *64A*, 73.
(17) Price, F. P. *J. Chem. Phys.* **1959**, *31*, 1679.
(18) Wunderlich, B. *Macromolecular Physics*; Academic: New York, 1973; Vol. I, p 388.
(19) Hock, C. W. *J. Polym. Sci.: B* **1965**, *3*, 573; *J. Polym. Sci.: A-2* **1966**, *4*, 227.
(20) Randall, J. C. *J. Polym. Sci., Polym. Phys. Ed.* **1976**, *14*, 2083.
(21) Cella, R. J. *J. Polym. Sci., Symp.* **1973**, *42*, 737.
(22) Buck, W. H.; Cella, R. J.; Gladding, E. K.; Wolfe, J. R. *J. Polym. Sci., Symp.* **1974**, *48*, 47.
(23) Cella, R. J. *Encyclopedia of Polymer Science and Technology*; John Wiley and Sons: New York, 1977; Supplement Vol. 2, p 485.

Laser-Pulsed Photopolymerization of Methyl Methacrylate: The Effect of Repetition Rate

Charles E. Hoyle,* M. A. Trapp, C. H. Chang, D. D. Latham, and Kevin W. McLaughlin

Department of Polymer Science, University of Southern Mississippi, Hattiesburg, Mississippi 39406-0076. *Received September 12, 1988; Revised Manuscript Received January 31, 1989*

ABSTRACT: The photopolymerization of neat methyl methacrylate at several different photoinitiator optical densities has been completed using a pulsed excimer laser. The operation of the laser was controlled using a microcomputer with the capability of firing the laser in two different modes. The first mode (single-pulse mode) was a continuous pulsing with each pulse separated by a 10-s time interval. This gave, upon GPC analysis, a broad molecular weight distribution. The second mode of pulsing (double-pulse mode), a sequence of two pulse blocks with a time between pulses of 100 ms and a time between the blocks of 10 s, gave a complex distribution characterized by a narrow shoulder superimposed on a broad molecular weight distribution. Both distributions can be described by employing the use of generating functions to solve the basic kinetic equations of polymerization.

Introduction

There has been a recent surge of interest in the use of lasers as a source to initiate free-radical polymerization processes.[1-31] Experiments have been directed at using lasers as both unique flash lamp sources to gain critical information dealing with the kinetics of free-radical polymerization processes and as a basic evaluation of laser sources as means of generating polymers with specific properties. In view of the obvious interest in laser-initiated polymerization processes, it is worthwhile to consider the kinetics of the polymerization and the molecular weight distributions derived therefrom.

Olaj and co-workers[8-12] have presented an evaluation of the rate constants of styrene using a "pseudostationary" approximation to describe the polymerization process. In this paper, we present experimental results for the laser-initiated polymerization of neat methyl methacrylate under a variety of considerations. By operation of the laser in both a "single-pulse" and "double-pulse" mode, two distinct and quite different molecular weight distributions are produced. The shape of the distributions are described

* Author to whom correspondence should be directed.

0024-9297/89/2222-3866$01.50/0

by solving the basic equations for free-radical polymerization using generating functions. The equations derived from this treatment are used to simulate the experimental data.

Experimental Section

Methyl methacrylate (MMA) (Aldrich) was passed through an inhibitor-removing column (DHR-4), supplied by Scientific Polymer Products, prior to use. The photoinitiator, 2,2-dimethoxy-2-phenylacetophenone (Irgacure 651 from Ciba-Geigy), was recrystallized several times from methanol. The concentration of the photoinitiator was varied to obtain several different absorbance values at λ = 350 nm. The absorbance was measured using a Perkin-Elmer Model 320 spectrophotometer. Samples (2 mL) of the neat (9.35 M) MMA were added to a 1-cm quartz cell. Each sample was purged with nitrogen for 10 min prior to exposure to the laser. Degassing with nitrogen was continued throughout the polymerization process.

The laser used was a Lumonics HyperEx-440 excimer laser operated with a xenon–fluorine fill gas mixture (output at 351 nm). The repetition rate and the number of pulses delivered were controlled using an IBM-XT PC as a triggering device. Conventional ferrioxalate actinometry was used to quantify the number of photons absorbed by the sample.[32,33] Each sample was exposed to approximately 2.0×10^{18} photons. After exposure the samples were analyzed using gel permeation chromatography (GPC).

The GPC system (35 °C) consists of a Waters (6000 psi) solvent delivery pump, a Model 7010 Rheodyne injector with a 50-μL injection loop, a Waters 410 differential refractometer, and three Ultrastyragel (Waters) columns (500, 10^3, and 10^4 Å) enclosed in a Waters column heater with a tetrahydrofuran mobile phase of 1 mL/min. The GPC system was calibrated using narrow molecular weight PMMA standards from Scientific Polymer Products. The following elution volumes (V_e) were obtained using several different molecular weight standards: M_w = 840 000, V_e = 17.70 mL; M_w = 502 200, V_e = 18.30 mL; M_w = 261 600, V_e = 18.90 mL; M_w = 107 000, V_e = 19.80 mL; M_w = 98 000, V_e = 19.90 mL; M_w = 30 000, V_e = 21.60 mL.

Results and Discussion

The data will be presented in two distinct sections, each designed to illustrate a specific fundamental characteristic of laser-initiated polymerization. The first section describes the results of polymerization initiated by single laser pulses (~10-ns fwhm) spaced at 10-s intervals. Operation in this single-pulse mode allows for chains initiated by one laser pulse to grow to completion prior to firing the next pulse. The second section involves firing the laser in a two-pulse or double-pulse mode with the first laser pulse followed by a second pulse 0.1 s later. A delay of 10 s elapses before the double-pulse sequence is repeated. The results from both the single-pulse and double-pulse modes are important in describing fundamental kinetic concepts inherent in photopolymerization initiated with a pulsed laser source.

Single-Pulse Mode. In the single-pulse mode, the laser is operated by firing at pulse intervals of 10 s (0.1 Hz) between pulses. In each case, 200 pulses are fired into a quartz cell containing a neat degassed methyl methacrylate (sample exposed through a solid disk with a 0.211-cm-diameter hole designed to exclude excess light from reaching the sample). From chemical actinometry it was determined that each sample was exposed to 2.0×10^{18} photons. The number of photons actually absorbed was obtained by knowing the absorbance of the photoinitiator.

Figure 1 shows the GPC results for the polymerization of neat MMA (9.35 M) with four photoinitiator absorbances at 351 nm ranging from 0.005 to 0.823. Several general observations based on these results can be made.

First, each of the molecular weight distributions is quite broad. This may be due in very limited part to a tendency

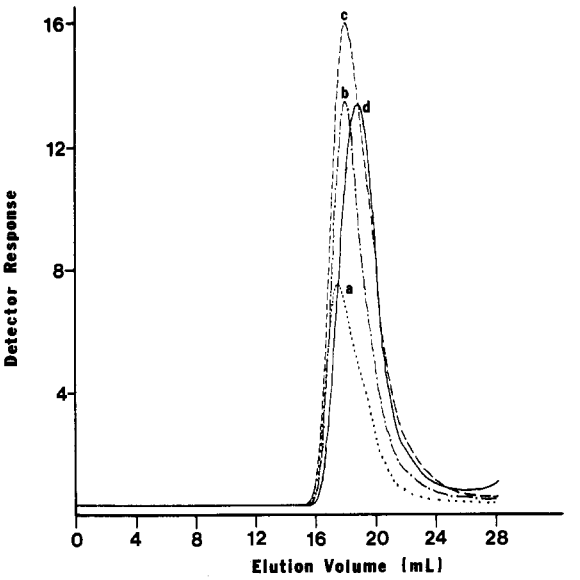

Figure 1. GPC chromatograms of poly(methyl methacrylate) generated by firing the laser with a repetition rate of 0.1 Hz (10 000 ms between pulses) for different photoinitiator optical densities: (a) OD = 0.005 (···); (b) OD = 0.031 (-·-); (c) OD = 0.250 (--); (d) OD = 0.823 (—).

for polymer radicals produced in the beam to diffuse into the unexposed medium during the course of polymerization. As will be noted in our theoretical description of laser-induced polymerization, a broad molecular weight distribution from operation in the single pulse mode is to be expected.

Second, there is an apparent shoulder on the low molecular weight side in each of the GPC curves in Figure 1, which is most pronounced for curve a (absorbance 0.005). This may be due to the well-known decrease in the rate constant for termination with polymer chain length [up to a degree of polymerization (DP) of about 1000 (34)]. The higher rate constant for chain termination would yield an unsymmetrical molecular weight distribution with an excess (shoulder) of low molecular weight species. At higher photoinitiator concentrations (curves b–d), the higher molecular weight species cannot form as a result of enhanced radical–radical recombination. Thus, at higher optical densities (OD) where the yield of primary radicals is quite large, most if not all of the growing polymer chains are terminated before obtaining degrees of polymerization much greater than 1000. At higher photoinitiator concentrations (Figure 2; absorbance 6.92), a significant fraction of the chains terminate before obtaining a high DP, and the GPC curve converges to a maximum DP of approximately 1000.

In Figure 3, a log–log plot of the photoinitiator optical density versus total integrated area (area) under the GPC curves in Figure 1 (as well as similar data obtained for several other photoinitiator concentrations) is characterized by a maximum at about –0.2 corresponding to an OD of about 0.6. The decrease in the conversion efficiency at higher photoinitiator absorbances can be attributed to a marked decrease in the quantum yield (Table I) for the propagation step (defined as the ratio of the moles of monomer polymerized to the moles of photons absorbed by the photoinitiator) with increasing photoinitiator concentration. Therefore, even though a larger number of photons are absorbed at higher optical densities, they are less effective in generating long kinetic chain lengths. The reduction in quantum yield with increasing concentration is due to increased radical–radical coupling resulting from the higher radical concentrations.

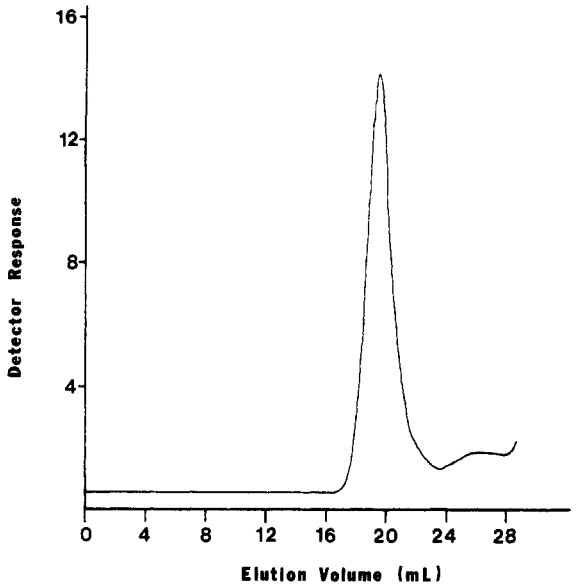

Figure 2. GPC chromatogram of poly(methyl methacrylate) generated by firing the laser with a repetition rate of 0.1 Hz (10000 ms between pulses) for a photoinitiator optical density equal to 6.92.

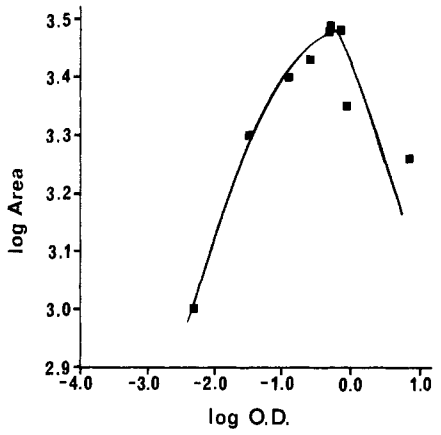

Figure 3. Plot of log area versus log OD for poly(methyl methacrylate) generated by firing the laser with a repetition rate of 0.1 Hz (10000 ms between pulses) for several different photoinitiator optical densities.

Table I[a]

OD	log OD	Φ	log Φ
0.005	−2.30	6548	3.82
0.031	−1.51	2130	3.33
0.123	−0.91	752	2.88
0.250	−0.60	449	2.65
0.450	−0.35	334	2.52
0.500	−0.30	327	2.51
0.692	−0.16	276	2.44
0.823	−0.08	194	2.29
6.920	0.84	135	2.13

[a] Optical densities and their corresponding quantum yields generated from a constant laser repetition rate of 0.1 Hz (10000 ms between pulses).

In order to describe the origin of the molecular weight distribution produced from the single-pulse polymerizations in Figure 1, a general mechanism for photopolymerization in the absence of steady-state radical concentration must be adopted. Scheme I depicts a typical scheme for free-radical polymerization initiated by absorbance of light (step 1) by a photoinitiator (PI) to give a pair of radicals (X• and W•). In order to be complete, consideration is given to the fact that both of the radicals

Scheme I

Initiation: $I \xrightarrow{h\nu} X^\bullet + W^\bullet$

Propagation: $X^\bullet + M \xrightarrow{k_p} XM_1^\bullet$

$XM_1^\bullet + M \rightarrow XM_2^\bullet$

$\vdots$

$XM_{i-1}^\bullet + M \xrightarrow{k_p} XM_i^\bullet$

Termination: $XM_i^\bullet + W^\bullet \xrightarrow{k_t} XM_iW$

$XM_{i-j}^\bullet + XM_j^\bullet \xrightarrow{k_t} XM_iX$

where $i > 0$ and $0 \leq j < i$

generated may not be equally effective in initiating the polymerization process; i.e., the W• radicals are simply effective chain terminators. In Scheme I, the species $XM_i^\bullet$ represents a living polymer chain with a degree of polymerization i initiated by the reactive X• radicals, which can be terminated by either $XM_j^\bullet$ or W•. In addition XM_iX and XM_iW represent the dead polymers with a degree of polymerization i, which are initiated by X• and terminated by $XM_j^\bullet$ or W•, respectively. For simplification $XM_i^\bullet$, XM_iX, and XM_iW are designated A_i, B_i, and C_i (see Scheme I). Equations for formation of the dead polymers B_i and C_i and the living polymer A_i are given in eq 1–3.

$$\frac{dA_i}{dt} = k_pA_{i-1}[M] - k_pA_i[M] - k_tA_i\sum_{j=0}^{\infty}A_j \quad (1)$$

$$\frac{dB_i}{dt} = \frac{1}{2}k_t\sum_{j=0}^{i}A_jA_{i-j} \quad (2)$$

$$\frac{dC_i}{dt} = k_t[W^\bullet]A_i \quad (3)$$

Equations 1–3 have been solved in terms of A_i (eq 4), B_i (eq 5), and C_i (eq 6) by the use of generating functions,[35] and only the results are shown. where

$$A_i = \frac{1}{2}\left(\frac{[R^\bullet]_0}{1 + k_t[R^\bullet]_0t}\right)\left(\frac{\gamma^ie^{-\gamma}}{i!}\right) \quad (4)$$

$$B_i = \frac{k_t}{8}\int\left(\frac{[R^\bullet]_0}{1 + k_t[R^\bullet]_0t}\right)^2\left(\frac{(2\gamma)^ie^{-2\gamma}}{i!}\right)dt \quad (5)$$

$$C_i = \frac{k_t}{4}\int\left(\frac{[R^\bullet]_0}{1 + k_t[R^\bullet]_0t}\right)^2\left(\frac{\gamma^ie^{-\gamma}}{i!}\right)dt \quad (6)$$

i = the degree of polymerization

$\gamma = k_p[M]t$ = average kinetic chain length of the living polymer chains

$[R^\bullet]_0$ = total radical concentration in polymerizing medium at time $t = 0$ following initiation by the laser pulse

The integrands in eq 5 and 6 represent a Poisson type distribution modified by a decay in the total radical concentration with time. Since in the single-pulse experiments it is only possible to obtain experimentally the dead polymer distribution, discussion of the significance of eq 4 will be postponed until the next section. For the present single-pulse case we contend that distributions described by eq 5 and/or 6 is tantamount to the integration of a Poisson function from the initial firing of the laser pulse (time zero) until all of the radicals present in the polymerizing system have been effectively terminated. Thus,

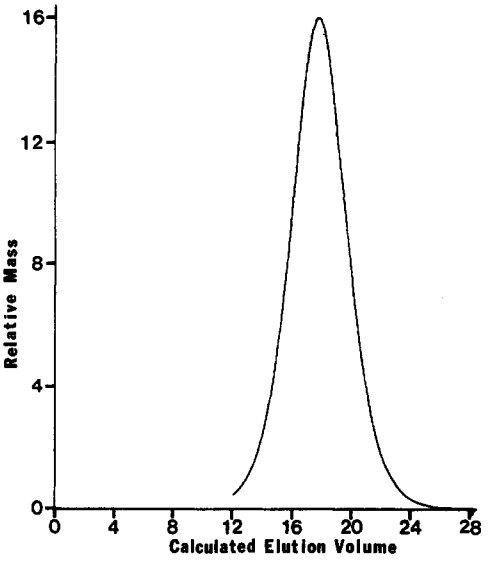

Figure 4. Computer-simulated GPC chromatogram of a broad molecular weight distribution for a laser repetition rate of 0.1 Hz (10 000 ms between pulses).

quite a broad distribution peak is to be expected. Figure 4, shows a distribution described by eq 5 and 6. Figure 4 shows the sum of the numerical integrations of eq 5 and 6. For this calculation $[M]k_p/[R^\bullet]_0k_t$ was taken to be 5000 and the initial concentration of radicals, $[R^\bullet]_0$, was arbitrarily fixed. The resulting distribution was converted into elution volume by use of a linear calibration curve, which related the elution volume to log molecular weight. The major feature of the simulation in Figure 4 is its broadness, which is comparable to the experimental GPC curve in Figure 1. (As pointed out in our previous discussion, the experimental GPC curve is characterized by a shoulder on the low molecular weight side due most likely to the decrease in k_t with increasing kinetic chain length below a degree of polymerization of 1000.) Thus, the distribution functions of eq 5 and 6 provide a logical description of the polymer generated by single laser pulses spaced at intervals large enough to allow a significant fraction of free-radical species to be terminated. The following section describes results of experiments in which the living polymer chains are prematurely terminated by a subsequent laser pulse (fired after the initial pulse) occurring at time intervals in which polymer chains are still propagating.

Double-Pulse Mode. In the double-pulse mode, the laser is rapidly pulsed at a 0.1-s interval followed by a 10-s delay before the sequence (i.e. firing of two pulses at a 0.1-s interval) is repeated. The process is repeated 100 times, thereby subjecting the sample to a total of 200 pulses; consequently, the same number of total photons (obtained by chemical actinometry) are delivered to the sample as in the single-pulse experiment. Figure 5 shows the GPC traces of the polymers produced from four (curves a–d) double-pulse experiments with photoinitiator absorbances ranging from 0.005 to 0.823. As the photoinitiator concentration increases, a distinct and very narrow peak is superimposed on a broad distribution. In each case the broad peak at higher molecular weight is essentially identical in shape to the distribution for the single-pulse experiments in Figure 1. These results are not surprising since in each case radicals generated by firing the second pulse (0.1 s after the first pulse) are able to initiate new polymer radicals as well as terminate the living polymer chains initiated by the first pulse. In other words, the second pulse in the sequence produces a large pool of primary radicals, which are available to quench or terminate the polymer radicals initiated by the first pulse (which are still living) and to initiate new polymer radicals. Since there is a 10-s delay after firing the second pulse before another laser pulse is fired, polymer chains produced by the second pulse should yield a molecular weight distribution essentially identical with the single-pulse distributions in Figure 1. This is certainly observed in Figure 5.

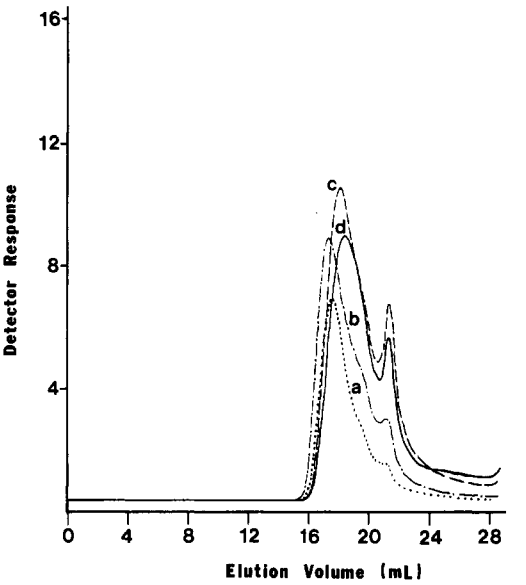

Figure 5. GPC chromatograms of poly(methyl methacrylate) generated by firing the laser with a two-pulse sequence. The repetition rate between pulse pairs was 10 Hz (100 ms), and the time between each two-pulse sequence was 0.1 Hz (10 s) for several different photoinitiator optical densities: (a) OD = 0.005 (···); (b) OD = 0.031 (-·-); (c) OD = 0.250 (--); (d) OD = 0.823 (—).

Table II[a]

OD	log OD	Φ	log Φ
0.005	−2.30	5791	3.76
0.031	−1.51	1553	3.19
0.123	−0.91	550	2.74
0.250	−0.60	350	2.54
0.480	−0.32	210	2.32
0.823	−0.08	155	2.19
6.920	0.84	69	1.84

[a] Optical densities and their corresponding quantum yields generated by firing the laser in the two-pulse mode.

The effect of photoinitiator concentrations, as reflected in curves a–d (Figure 5), is multifold. As the absorbance of the photoinitiator increases, the overall polymer yield increases (curves a–c) at low concentrations (OD < 0.25) followed by a decrease at higher concentrations (see curve d, Figure 5 for 0.823 absorbance). This is the same general trend noted in Figure 1. The most pronounced photoinitiator effect, however, is the growing in of the narrow peak at lower molecular weights with increasing concentration (absorbance). Apparently, at low photoinitiator concentration (curve a), the concentration of primary radicals from the second pulse is barely sufficient to terminate the living polymer radicals from the first pulse and only a small "bump" can be seen on the low molecular weight side of the broad main peak. At higher concentrations the sharp peak at low molecular weights is quite pronounced.

As in the case of the single-pulse experiments, the quantum yield for polymer formation is significantly diminished at higher photoinitiator concentrations (see Table II). Interestingly, the slope of the log–log plot of the quantum yield (Φ) versus absorbance of the double-pulse experiment shown in Figure 6 (plotted from Table II for

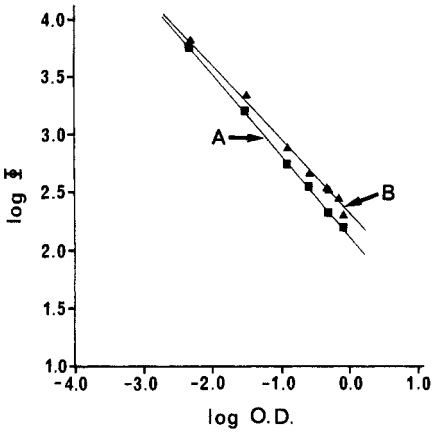

Figure 6. log–log plot of quantum yield versus optical density for poly(methyl methacrylate) generated by firing the laser in the (A) 0.1-Hz, 10-Hz double-pulse mode and (B) 0.1-Hz single-pulse mode.

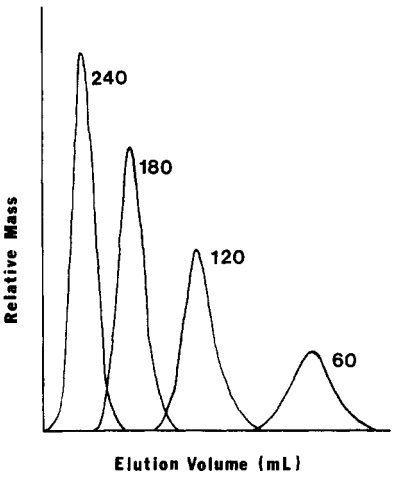

Figure 7. Computer-simulated GPC plot for the living polymer as calculated by eq 4, for γ = 60, 120, 180, and 240.

OD 0.005–0.823) is larger than the slope for the single-pulse experiment. This certainly is reasonable since premature termination of polymer radicals from the first pulse would result in lower overall monomer consumption. Note that at low photoinitiator concentrations the plots in Figure 6 should intersect. The concentration corresponding to this intersection represents the minimum concentration in the double-pulse experiment required to produce enough primary radicals to effect chain termination.

The origin of the narrow molecular weight distribution peak at an elution volume of 21.32 mL in Figure 5 can be understood, as already discussed at length, as resulting from premature termination of the living polymer chains by interjection of the "second" pulse. Such an argument was presented by Olaj et al. to account for the narrow peak superimposed on a broad distribution from the laser-initiated polymerization of styrene.[8-11] What follows is an attempt at a direct kinetic solution to an interpretation of the results in Figure 5 and thus a mechanistic rationale for the double-pulse experiment. Equation 4 defines the distribution of the living polymer. This equation can be described as a Poisson distribution modified by a factor that accounts for the decay of free-radical species with time. Figure 7 shows the relative mass versus elution volume as described by eq 4, for times corresponding to γ = 60, 120, 180, and 240. For this figure $[M]k_p/[R^\bullet]_0k_t$ was taken to be 350, and the value of $[R^\bullet]_0$ was chosen arbitrarily. It can be seen, from Figure 7, that the living polymer generated by the first pulse shifts to higher molecular weight as time increases. When a second pulse is fired at a particular delay time (in our experimental case, 0.1 s) after the first pulse, a portion of the living polymers are immediately terminated by infusion of small molecular (primary) radicals. Assuming that the primary radicals combine statistically, i.e., independent of the molecular weight of the living polymer radicals, then a narrow peak in the molecular weight distribution curve of the polymers produced should be described by a narrow distribution peak similar to one of those shown in Figure 7. This peak will be superimposed on the broad distribution produced by the polymer chains initiated by the second pulse in each sequence as well as those chains produced by the first pulse in each sequence which are not terminated by primary radicals from the second pulse. The result is essentially a combination of the living peak (as simulated in Figure 7) superimposed on the broad peak (as simulated in Figure 4). This of course results in a distribution that has all of the structural details of the experimental chromatograms in Figure 5.

Conclusions

The results in this paper illustrate the effect of photoinitiator concentration and pulsing sequence on the polymers generated from the laser-initiated polymerization of methyl methacrylate. At low photoinitiator concentrations, operation in the single-pulse mode results in a sample with an extremely broad molecular weight distribution. A distinct shoulder on the low molecular weight side is presumably due to the variance in the termination rate constant with polymer kinetic chain length. The quantum efficiency of the polymerization decreases significantly with increasing photoinitiator concentration resulting in a loss of higher molecular weight species. In the double-pulse mode a combination of two pulses at close interval (0.1 s) are delivered to the neat sample followed by a delay of 10 s. The double-pulse experiment is characterized by the appearance of a modified Poisson distribution superimposed on a broad molecular weight distribution. The sharp Poisson peak is interpreted in terms of a living radical distribution, which has been quenched or "frozen" as a result of the small molecule radicals produced by the second laser pulse in the series. By comparison of the quantum efficiencies of polymerization for the single- and double-pulse experiments as a function of the photoinitiator absorbance, a threshold absorbance required to terminate growing polymer radicals is estimated.

Finally, a set of theoretical equations derived from the basic kinetic equations for free-radical polymerization have been effectively utilized to describe the laser-initiated polymerization of methyl methacrylate under two sets of laser operating parameters. Subsequent papers in this series will deal with the effect of operating the laser at a whole series of repetition rates ranging from low to high pulsing frequencies.

Acknowledgment. This research is supported by National Science Foundation Grant DMR 85-14424 (Polymers Program). Acknowledgment is also made to NSF for assistance in purchasing the laser system utilized in the course of this investigation (Grant CHE-8411829 Chemical Instrumentation Program).

Registry No. MMA, 80-62-6; MMA (homopolymer), 9011-14-7; Irgacure 651, 24650-42-8.

References and Notes

(1) Decker, C. *J. Polym. Sci., Polym. Chem. Ed.* **1983**, *21*, 2451.
(2) Decker, C. *J. Coat. Technol.* **1984**, *56*, 29.
(3) Decker, C. *Polym. Prepr.* **1984**, *25*, 303.
(4) Decker, C. *ACS Symp. Ser.* **1984**, *266*, 207.

(5) Decker, C. *Polym. Mater. Sci. Eng.* **1983**, *49*, 32.
(6) Decker, C.; Moussa, K. *Polym. Mater. Sci. Eng.* **1986**, *55*, 552.
(7) Decker, C. *Radcure Proceedings* **1983**, FC 83-265.
(8) Olaj, O. F.; Bitai, I.; Kauffmann, H. F.; Gleixner, G. *Oesterr. Chem. Z.* **1983**, *84*, 264.
(9) Olaj. O.; Bitai, I.; Gleixner, G. *Makromol. Chem.* **1985**, *186*, 2569.
(10) Olaj, O.; Bitai, I.; Hinkelmann, F. *Makromol. Chem.* **1987**, *188*, 1689.
(11) Olaj, O.; Bitai, I. *Angew. Makromol. Chem.* **1987**, *155*, 177.
(12) Olaj, O.; Bitai, I. *Makromol. Chem., Rapid Commun.* **1988**, *9*, 275.
(13) Fouassier, J. P.; Jacques, P.; Lougnot, D. J.; Pilot, T. *Polym. Photochem.* **1984**, *5*, 57.
(14) Fouassier, J. P.; Lougnot, D. J.; Pilot, T. *J. Polym. Sci., Polym. Chem. Ed.* **1985**, *23*, 569.
(15) Fouassier, J. P.; Lougnot, D. J. *Makromol. Chem.* **1983**, *4*, 11.
(16) Williamson, M. A.; Smith, J. D. B.; Castle, P. M.; Kauffman, R. N. *J. Polym. Sci., Polym. Chem. Ed.* **1982**, *20*, 1875.
(17) Sadhir, R. K.; Smith, J. D. B.; Castle, P. M. *J. Polym. Sci., Polym. Chem. Ed.* **1983**, *21*, 1315.
(18) Decker, C. Polym. *Photochem.* **1983**, *3*, 131.
(19) Decker, C. *Macromolecules* **1985**, *18*, 1241.
(20) Hoyle, C. E.; Hensel, R. D.; Grubb, M. B. *J. Polym. Sci., Polym. Chem. Ed.* **1984**, *22*, 1865.
(21) Hoyle, C. E.; Hensel, R. D.; Grubb, M. B. *J. Radiat. Curing*, **1984**, *11*(4), 22.
(22) Hoyle, C. E.; Hensel, R. D.; Grubb, M. B. *Polym. Photochem.* **1984**, *4*, 69.
(23) Sadhir, R. K.; Smith, J. D. B.; Castle, P. M. *J. Polym. Sci., Polym. Chem. Ed.* **1985**, *23*, 411.
(24) Hoyle, C. E.; Trapp, M. A.; Chang, C. H. *Polym. Mater. Sci. Eng.* **1987**, *57*, 579.
(25) Hoyle, C. E.; Chawla, C. P.; Chatterton, P. M.; Trapp, M. A.; Chang, C. H.; Griffin, A. C. *Polym. Prepr.* **1988**, *29*(1), 518.
(26) Hoyle, C. E.; Trapp, M. A.; Chang, C. H.; Latham, D. D.; McLaughlin, K. W. *Macromolecules* **1989**, *22*, 35.
(27) Hoyle, C. E.; Trapp, M. A.; Chang, C. H. *Macromolecules*, in press.
(28) Chin, S. L. *Can. J. Chem.* **1976**, *54*, 2341.
(29) Oraevskii, A. N.; Pimenov, V. P.; Stepanov, A. A.; Shcheglov, V. A. *Sov. J. Quantum Electron. (Engl. Transl.)* **1974**, *4*(5), 711.
(30) Aleksandrov, A. P.; Genkin, V. N.; Kital, M. S.; Smirnova, I. M.; Sokolov, V. V. *Sov. J. Quantum Electron. (Engl. Transl.)* **1977**, *7*(5), 547.
(31) Decker, C. In *Radiation Curing of Polymers*; Randell, D. R., Ed.; Royal Society of Chemistry: London, 1987; No. 64, p 16.
(32) Hatchard, C. G.; Parker, C. A. *Proc. R. Soc. London, A* **1956**, *235*, 518.
(33) Calvert, J. G.; Pitts, J. N. *Photochemistry*; Wiley: New York, 1966; pp 780–786.
(34) North, A. M. *Reactivity, Mechanism and Structure in Polymer Chemistry*; Wiley-Interscience: New York, 1974; Chapter 5, p 142.
(35) McLaughlin, K. W.; Latham, D. D.; Hoyle, C. E.; Trapp, M. A. *J. Phys. Chem.* **1989**, *93*, 3643.

New Copolymers of Styrene with Some Trisubstituted Ethylenes

Gregory B. Kharas*

Polysar Incorporated, Plastics Division, 29 Fuller Street, Leominster, Massachusetts 01453

Kenneth Watson

Polysar Limited, Sarnia, Ontario N7T 7M2, Canada. *Received July 7, 1988; Revised Manuscript Received March 3, 1989*

ABSTRACT: Novel trisubstituted ethylenes, 1,1-dicyanoethenes, methyl 2-cyanopropenoates, and 1,1-bis(methoxycarbonyl)ethenes, having cyclohexyl, 3-cyclohexenyl, 5-norbornenyl, phenyl, 1-naphthyl, 3-pyridinyl, 2-pyrrolyl, and 2-furyl substituents at the double bond have been prepared via Knoevenagel condensation of the corresponding aldehydes and active methylene compounds, malononitrile, methyl cyanoacetate, and dimethyl malonate. The trisubstituted ethylenes were copolymerized with styrene at equimolar monomer feed with the radical initiation. Relative reactivity of the trisubstituted ethylene monomers and radicals, estimated on the basis of the compositional data, increases in the same order as their acceptor properties: 1,1-dicyanoethenes > methyl 2-cyanopropenoates ≫ 1,1-bis(methoxycarbonyl)ethenes. 2-Pyrrolyl- and 2-furyl-substituted 1,1-dicyanoethenes, methyl 2-cyanopropenoates, and 1,1-bis(methoxycarbonyl)ethenes were unreactive in copolymerization with styrene.

Introduction

Early studies of substituted ethylenes showed that reactivity of the monomers in radical polymerization depends on their polarity, resonance stabilization, and steric effects.[1] 1,1-Disubstituted alkenes are generally more reactive than monosubstituted ethylenes due to resonance stabilization of the growing radical by both substituents. However, the ability of the monomer to polymerize is critically dependent on the bulkiness of the substituent, which leads to steric strain in the polymer and results in low ceiling temperatures.

1,2-Disubstituted ethylenes are significantly less reactive than the monosubstituted monomers. The propagation step is extremely slow due to steric interactions between the β-substituent of the propagating species and the two substituents of the incoming molecule.[1] Polymerization of trisubstituted ethylenes evidently should be further impeded on the grounds of both thermodynamic and kinetic factors encountered in the case of 1,1- and 1,2-disubstituted alkenes.

In copolymerization of trisubstituted ethylene monomers with monosubstituted olefins, influences due to steric hindrance are mostly minor compared to polarity and resonance stabilization.

Use of electron-deficient trisubstituted alkenes carrying two cyano, halo, and/or carboalkoxy substituents in copolymerization with electron-rich monosubstituted ethylenes made it possible to overcome steric problems observed in the homopolymerization.[2-4] Monomer polar interactions between dimethyl cyanofumarate or tricarbomethoxyethylene and α-methylstyrene, indene, furane, or benzofurane allowed even copolymerization of trisubstituted ethylenes with 1,1- and 1,2-disubstituted monomers.[5] On the other hand, in attempted copolymerization with monosubstituted comonomers of similar polarity such as methyl acrylate or acrylonitrile, these same trisubstituted carboxylate monomers gave no

* To whom correspondence should be addressed.

0024-9297/89/2222-3871$01.50/0